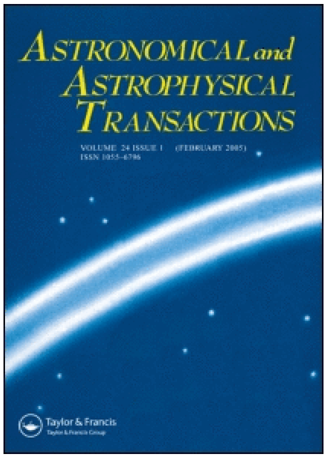

Astronomical & Astrophysical Transactions
The Journal of the Eurasian Astronomical Society
Publication details, including instructions for authors and subscription information:
http://www.informaworld.com/smpp/title~content=t713453505

The low-frequency radio recombination lines formed in the extremely extended C II regions

N. I. Rovenskaya [a]
[a] Institute of Radio Astronomy, Kharkiv, Ukraine

Online Publication Date: 01 August 2007
To cite this Article: Rovenskaya, N. I. (2007) 'The low-frequency radio recombination lines formed in the extremely extended C II regions', Astronomical & Astrophysical Transactions, 26:4, 203 - 209
To link to this article: DOI: 10.1080/10556790601135406
URL: http://dx.doi.org/10.1080/10556790601135406

Astronomical and Astrophysical Transactions
Vol. 26, Nos. 4–5, August–October 2007, 203–209

Taylor & Francis
Taylor & Francis Group

The low-frequency radio recombination lines formed in the extremely extended C II regions

N. I. ROVENSKAYA*

Institute of Radio Astronomy, 4 Chervonopraporna Street, Kharkiv 61002, Ukraine

(Received 11 October 2006)

Currently, nearly ten radio recombination lines are observed in the extremely extended C II regions towards Cassiopeia A, G00-00, G05-00 and G10-00. The centimetre linewidths are formed owing to the Doppler effect. The decametre linewidths are the result of combinations of the Doppler broadening, radiation interaction and electron collision transition rate. The electron collision width is determined in the impact approximation, which can be employed for highly excited atom states with the principal quantum and line numbers n in the case when $1.6 \times 10^5\ \mathrm{K}/n^2 T_e \ll 1$, $n > 500$. The decametre linewidth components are tabulated together with the calculated electron densities. The dimensions of the C II regions are directly determined by using the steep dependence of the optical depth of a centimetre recombination line on the electron temperature. Solving the optical depth problem and having accounted for the spontaneous and collision transition rates in the balance equations, the highly excited atom non-equilibrium radiation lines and populations are found as functions of the principal quantum numbers in the diffusion or flux form solution approximation. The centimetre and decametre lines observed and interpreted show that the C II regions may have huge dimensions and extremely low electron densities.

Keywords: Low-frequency recombination line; Highly excited carbon atom; Extremely extended C II region

1. Introduction

The carbon low-frequency radio recombination lines $C_{201\alpha}$–$C_{686\alpha}$ and $C_{732\beta}$–$C_{868\beta}$ form in the extremely extended C II regions. These lines originate as a result of the transition from the highly excited carbon atom states with principal quantum numbers that are equal to those of the lines. The low-frequency lines result from the regions with low emission measures of less than $1\ \mathrm{cm}^{-6}$ pc, and the velocities of the regions are directly determined experimentally. Analysing the centimetre, metre and decametre radio recombination line data in detail, the densities and dimensions of the C II regions may be determined to enable further studies of the origin of the C II regions to be made.

*Email: rai@ira.kharkov.ua

Astronomical and Astrophysical Transactions
ISSN 1055-6796 print/ISSN 1476-3540 online
http://www.tandf.co.uk/journals
DOI: 10.1080/10556790601135406

From theoretical models, the extended and compact C II regions originate from gas interaction with ultraviolet radiation of wavelengths $\lambda > 912$ Å from the H II regions. These C II regions are known as photodissociation regions [1–6].

So, the compact and extended C II regions are now studied. Here the new physics of the C II regions observed in the low-frequency range are presented. These regions have huge dimensions compared with those of the Galactic arm. The electron densities found using the linewidth interpretation are much smaller than those of the extended C II regions. The electron temperatures are much higher than those found in the extended C II regions.

The lowest-frequency carbon radio recombination lines were first detected as early as 1979. In further experiments, more than 50 lines were observed from 1984 to 2001 in the extremely extended C II region towards Cassiopeia A. The centimetre and decametre lines have been observed since 2000 in the Galactic plane C II regions. The carbon centimetre radio recombination lines $C_{201\alpha}$–$C_{270\alpha}$ are broadened owing to the Doppler effect. The lowest-frequency lines are broadened because of a combination of the Doppler, radiation and collision broadening effects. Since the Doppler linewidth component is experimentally found and the radiation-induced linewidth component is calculated for the radiation temperature measured, the collision linewidth component can be determined and the electron volume density may be theoretically calculated in the impact approximation, which can be employed in the case when $1.6 \times 10^5\,\mathrm{K}/n^2 T_e \ll 1$, $n > 500$.

Interpreting the experimental intensity values of the radio recombination lines $C_{201\alpha}$–$C_{229\alpha}$ may allow fairly accurate determination of the dimensions of the C II regions, if the temperatures of these regions are taken to be within the range $T_e = 200$–400 K. The current experiments are being carried out with the UTR-2 (Kharkiv, Ukraine), DKR-1000 (Puschino, Russia), Giant Metrewave Radio Telescope (India) and National Radio Astronomy Observatory (USA) instruments [7–13].

This paper aims to study the physical conditions in the extremely extended C II region by analysing the linewidths and line intensities. The lines $C_{630\alpha}$–$C_{868\beta}$ are broadened owing to the Stark effect [9, 14], since a highly excited carbon atom has a large dimension and a collision interaction cross-section $\Delta\nu^C \propto n^4$, $n \geq 600$, where $\Delta\nu^C$ is the linewidth. When the electron density has been found and the $C_{270\alpha}$–$C_{273\alpha}$ line intensity data have been interpreted, the dimensions of the C II regions can be approximately determined [11].

The carbon ion density is assumed to be equal to that of the electron volume and can be determined using the linewidth component interpretation of the carbon radio recombination lines $C_{570\alpha}$–$C_{868\beta}$. Recombination line collision broadening has been studied in [15–22] and interpreted in [14]. The collision cross-sections are determined in the so-called high-temperature or impact approximation, which is employed when $1.6 \times 10^5\,\mathrm{K}/n^2 T_e \ll 1$, $n \geq 600$. The collision widths are calculated by utilizing a dynamic model of a highly excited atom and scattering electron in which the dipole interaction approximation can be accepted with very high accuracy. For highly excited states with the principal quantum and line numbers n, the highly excited state electron velocity is much smaller than that of a free electron, $v_0/nv \ll 1$, $v_0 = 2.18 \times 10^8\,\mathrm{cm\,s^{-1}}$, and the collision dynamic problem is solved using the perturbation theory approximation given in [14, 16, 17]. From these papers and having interpreted the lowest-frequency radio recombination collision linewidth component, the electron volume density can be determined with the accuracy of $\delta = 0.2$. So, in this paper the action with the following dipole interaction potential is considered: $(1/\hbar)\int_{-\infty}^{\infty} V^{\mathrm{dip}}\,\mathrm{d}t \ll 1$. In some papers this integral is considered to be more than one; in the latter asymptotic case, the cross-section formula should describe the multiple-resonance case, and it is evident that the collision cross-section is much simpler for the highly excited atom than in this latter case.

To determine theoretically the dimensions of the C II regions, the centimetre line non-equilibrium intensities are studied as functions of the electron temperature. To consider this problem, the highly excited atom balance equations are analytically solved for the b_n factors, which are the factors of departure from the local thermodynamic equilibrium populations. There exist numerical and analytical approaches to the determination of the atomic population [18, 23–25]. The collision and spontaneous transition rates are accounted for in the population balance equations. The right-hand side of the balance equation represents photorecombination. The integral balance equation can be written in the diffusion form owing to the transitions to the nearest states [25]. The non-equilibrium coefficient has a very simple flux form in this case: $n \gg 1$, $\partial b_n/\partial n \propto 1/n^7$. This solution agrees well with that of the numerical approach [23, 24]. The non-equilibrium coefficients found are used with the centimetre recombination line interpretation. To explain the emission line observations, the electron temperatures T_e are chosen to be more than or equal to 200 K. To calculate the dimensions of the C II regions as a function of temperature, the experimental data are taken from [11, 13].

There are four sections in this paper. Section 2 is devoted to the interpretation of the radio recombination linewidths for states with $n = 570$–580 and the densities of the C II regions. The recombination line populations and optical depths are determined in section 3. Section 4 is devoted to conclusions.

2. The electron densities of the extremely extended C II regions as a result of the interpretation of the radio recombination linewidths

To determine the electron densities of the extended C II regions towards Cassiopeia A, G00-00, G05-00 and G10-00, let us analyse the metre and decametre linewidth data presented in [7–13]. The decametre radio recombination linewidth is a combination of the Doppler, radiation interaction and collision broadening effects. Since the Doppler and radiation interaction width components are measured independently in centimetre experiments, the collision width component can be calculated and the electron density found from experiments. The results of the collision width determination are listed later in table 1. To calculate the electron density, the collision width can be described using the impact approximation studied theoretically in [14–17, 21, 22].

The Doppler and background radiation linewidth components are calculated from the experimental data given in [10–13]. The centimetre lines $n = 291$–221 and $n = 270$–273 are narrow owing to the Doppler effect. The radiation interaction width can be calculated, since the radiation temperature is measured in the experiments and determined to be $T_R = 800 \pm 100$ K [11]. Evaluating the Doppler and radiation linewidths from the formulae in [18], the collision width component can be determined from the effective width formula given in the same paper as

$$\Delta\nu_L = [(\Delta\nu^D)^2 + (\Delta\nu^{BG} + \Delta\nu^C)^2]^{1/2}, \quad (1)$$

where $\Delta\nu_L$ is the linewidth, $\Delta\nu^D$ is the Doppler linewidth, $\Delta\nu^{BG}$ is the linewidth due to the radiation interaction and $\Delta\nu^C$ is the collision width.

Table 1. The low-frequency line parameters.

	τ (10^{-4})	$\Delta\nu_L$ (km s^{-1})
G00−00	2.0	20.5
G05+00	2.3	21.2
G10+00	2.0	37.5
Cas A	3.8	10.5

The background radiation interaction linewidth is determined by the formula in [18] as

$$\Delta\nu^{\mathrm{BG}} = 0.789 \times 10^{10} \frac{T_{\mathrm{R}}}{3.2 \times 10^{5}\,\mathrm{K}} (\mathrm{s}^{-1}), \quad T_{\mathrm{R}}|_{n=273} = 800\,\mathrm{K}, \tag{2}$$

where $\Delta\nu^{\mathrm{BG}}$ is the radiation interaction width, T_{R} is the background radiation temperature and n is the principal quantum and line number.

The collision width component can be described by the dipole interaction matrix element calculated with the second-order accuracy of the perturbation theory and averaged with a target distance and free-electron velocity; this dynamic equation solution is employed for the collision width calculation, if the highly excited electron velocity is much smaller than the free-electron velocity, $(v_0/nv)^2 \propto 1.6 \times 10^5\,\mathrm{K}/n^2T \ll 1$; the impact approximation condition and calculation accuracy have been discussed in [14–16, 21]. To find the electron volume density, the collision linewidth can be written as a function of the principal quantum number as follows:

$$a_{n,n+\Delta n} \propto \frac{r_{n,n+\Delta n}}{\rho}\frac{v_0}{nv}, \quad \frac{\omega_n \rho}{v} \ll 1,$$

$$W_n^{\mathrm{C}}(\Delta n) = \langle v\sigma_{n,n+\Delta n}\rangle,$$

$$\sigma_{n,n+\Delta n} = 2\pi \int_{\rho_0}^{\infty} \mathrm{d}\rho\, \rho a_{n,n+\Delta n}^2,$$

$$\begin{aligned}\Delta\nu^{\mathrm{C}} &= \sum_{\Delta n=1}^{\infty} W_n^{\mathrm{C}}(\Delta n)\\ &= \frac{4}{3}\left(\frac{1}{2\pi}\right)^{1/2} 1.18\, N_{\mathrm{e}} \left(\frac{m}{kT_{\mathrm{e}}}\right)^{1/2} \left(\frac{\hbar}{m}\right)^2 n^4 \left[\ln\left(\frac{n^2T_{\mathrm{e}}}{1.6 \times 10^5\,\mathrm{K}}\right) + \frac{1}{2}\right] (\mathrm{s}^{-1}),\\ &\frac{1.6 \times 10^5\,\mathrm{K}}{n^2T_{\mathrm{e}}} \ll 1,\end{aligned} \tag{3}$$

where $a_{n,n+\Delta n}$ is the dipole interaction matrix element, $r_{n,n+\Delta n}$ is the highly excited atom radius, ρ nd v are the scattering electron target distance and velocity respectively, $\sigma_{n,n+\Delta n}$ is the highly excited atom cross-section, $\Delta\nu^{\mathrm{C}}$ is the collision width, $W_n^{\mathrm{C}}(\Delta n)$ is the collision transition rate, n is the principal quantum and line number, N_{e} and T_{e} (K) are the electron volume density and temperature, respectively, m is the electron mass and k is the Boltzmann constant.

In table 1, the experimental linewidths $\Delta\nu_{\mathrm{L}}$ and optical depths τ are listed for $n = 273$.

In table 2, the Doppler width components $\Delta\nu^{\mathrm{D}}$ are calculated for the results using the data from [11, 13]. The background radiation width components $\Delta\nu^{\mathrm{BG}}$ are calculated for the radiation temperature $T_{\mathrm{R}} = 800\,\mathrm{K}$ found in the same paper. By using equations (1) and (3) the electron volume density N_{e} is calculated for the extremely extended C II regions.

Table 2. The calculated low-frequency linewidth components.

	$\Delta\nu^{\mathrm{D}}$ ($10^3\,\mathrm{s}^{-1}$)	$\Delta\nu^{\mathrm{BG}}$ ($10^3\,\mathrm{s}^{-1}$)	$\Delta\nu^{\mathrm{C}}$ ($10^3\,\mathrm{s}^{-1}$)	N_{e} ($10^{-2}\,\mathrm{cm}^{-3}$)
G00−00	0.47	0.042	2.25	1.8
G05+00	0.47	0.042	2.35	2.0
G10+00	0.47	0.042	4.24	3.5
Cas A	0.47	0.042	3.40	2.8

3. The dimensions of the extremely extended C II regions as functions of the recombination line intensities

To calculate the dimensions of the C II regions, the intensities of the lines $n = 270$–273 are studied as functions of the temperatures. The optical depth of the line can be calculated by the formula given in [18, 26], which is a function of the temperature and amplification coefficient. Let us write the optical depth of the line as

$$\begin{aligned} \tau_{n,n+\Delta n} &= 1.1 \times 10^{-3} \frac{f_{n,n+\Delta n}}{n} \left(\frac{10^4\,\mathrm{K}}{T_\mathrm{e}}\right)^{5/2} b_n \beta_n \frac{N_\mathrm{e}^2 R}{\pi^{1/2}\,\Delta\nu^\mathrm{D}}, \\ f_{n,n+\Delta n} &= 0.19n, \end{aligned} \tag{4}$$

where $\tau_{n,n+\Delta n}$ is the optical depth of the line n, which is known from experiments, R is the dimension of the C II region determined in parsecs and $b_n\beta_n$ is the line amplification coefficient. The other parameters are determined in equation (3).

The amplification coefficients are found from the balance equation solutions calculated analytically; the balance equations are written as follows [15, 18, 24]:

$$\begin{aligned} &\sum_{\Delta n=1} A_{n+\Delta n,n} b_{n+\Delta n} - b_n \sum_{\Delta n=1} A_{n,n-\Delta n} + \sum_{\Delta n=-1}^{\Delta n=+1} W^\mathrm{C}_{n+\Delta n,n} b_{n+\Delta n} - b_n \sum_{\Delta n=-1}^{\Delta n=+1} W^\mathrm{C}_{n,n+\Delta n} \\ &\quad = \frac{1}{n^3} \left\langle v\sigma_n^\mathrm{rec} \right\rangle \left(\frac{T_\mathrm{e}}{1.6 \times 10^5\,\mathrm{K}}\right)^{3/2} \frac{1}{N_\mathrm{e} a_0^3}. \end{aligned} \tag{5}$$

The amplification coefficient is found in the balance equation diffusion approximation [24, 25]:

$$\begin{aligned} \frac{\partial b_n}{\partial n} &= \left[\frac{1}{5n^5} \left\langle v\sigma_n^\mathrm{rec} \right\rangle \left(\frac{T_\mathrm{e}}{1.6 \times 10^5\,\mathrm{K}}\right)^{3/2} \frac{1}{N_\mathrm{e} a_0^3} + \frac{1}{n_1^2}\right] \left(\frac{1}{1 + D_n^C}\right), \\ D_n^\mathrm{C} &= \frac{n^3}{A_0} \sum_{\Delta n=1}^{\infty} \frac{(\Delta n)^2}{2} W^C_{n+\Delta n,n}, \quad A_0 = 0.789 \times 10^{10}\,(\mathrm{s}^{-1}), \\ & D_n^\mathrm{C}|_{n=n_1}. = 1, \\ b_n\beta_n &= b_n - \frac{T_\mathrm{e} n^3}{3.2 \times 10^5\,\mathrm{K}} \frac{\partial b_n}{\partial n}, \quad \frac{n^2 T_\mathrm{e}}{1.6 \times 10^5\,\mathrm{K}} \gg 1, \quad n \gg 1, \end{aligned} \tag{6}$$

where D_n^C is the diffusion factor, A_0/n^3 is the spontaneous transition rate and $\langle v\sigma_n^\mathrm{rec}\rangle$ is the photorecombination rate. The other coefficients are described in equations (3) and (4).

Equation (6) states that the amplification factor is inversely proportional to the electron flux and diffusion coefficient. The equation solution is the sum of the general and partial solutions, where $1/n_1^2$ is the constant for the general solution. For the temperature $T_\mathrm{e} = 200\,\mathrm{K}$ the amplification coefficients found analytically are smaller than those found numerically in [23]; these calculation differences are explained by the initial condition chosen in solution (6). It is probable that in the numerical solution the initial condition for the general solution is taken in the form $3/n_1^3$.

The dimensions of the C II regions are calculated using equations (4)–(6); these values are listed in table 3. Since the centimetre lines are observed in the emission spectra, the

Table 3. The dimensions of the C II regions.

	R (10^3 pc)	
	$T_e = 200\,\mathrm{K}$	$T_e = 400\,\mathrm{K}$
G00−00	0.40	0.96
G05+00	0.39	0.93
G10+00	0.14	0.56
Cas A	0.30	0.77

temperatures of the extremely extended C II regions should be high. In the second column of table 3 the electron temperature T_e is taken to be 200 K, and in the second column this value is taken to be 400 K.

The decametre line intensities are found to be due to dielectronic recombination and are formed in the absorption spectra; the highly excited atom populations are studied in this case and have some other population distributions described in [24, 27, 28]. The amplification coefficients are both the exponential and the power functions of the electron temperature, and the inaccuracy in the temperature calculation may be very large because of the form of the formula used.

4. Conclusions

The extremely extended C II regions are observed in the centimetre and decametre ranges. Owing to experiment interpretation it is found that C II regions may have the very large dimensions and low electron densities. Since the centimetre lines are detected in the emission spectra, it may be shown that the electron temperatures T_e of the C II regions are higher than 200 K.

The extended and compact C II region models have been described in [1–5, 29]. In these theoretical models, there are free parameters that may be determined more accurately. The hydrogen volume density is assumed to be in the wide range $10^2\,\mathrm{cm}^{-3} < N_\mathrm{H} < 10^6\,\mathrm{cm}^{-3}$ and the electron temperature calculated in the range $60\,\mathrm{K} < T_\mathrm{e} < 100\,\mathrm{K}$. These parameters are found from C II 158 μm line detection. Currently, the C II 158 μm fine-structure line is detected by the ISO experimental method [3].

In this paper the analytical analysis of the radio recombination linewidths and intensities is presented to determine the physical parameters of the C II regions. With this goal the electron densities are calculated using decametre radio recombination line collision broadening. The line intensities are used to explain the electron temperatures and dimensions.

Radio recombination lines are studied experimentally in a wide frequency range; there are the centimetre lines $\mathrm{C}_{201\alpha}$–$\mathrm{C}_{273\alpha}$, and the metre and decametre lines $\mathrm{C}_{570\alpha}$–$\mathrm{C}_{686\alpha}$ and $\mathrm{C}_{860\beta}$–$\mathrm{C}_{868\beta}$. These experiments have been carried out by the UTR-2 (Kharkiv, Ukraine), DKR-1000 (Puschino, Russia), Giant Metrewave Radio Telescope (India) and National Radio Astronomy Observatory (USA) instruments [7–13].

From experiments the lowest-frequency radio recombination lines are broadened owing to the Stark effect and the electron density is calculated as a result of the linewidth analysis. The determination of the accuracy of the electron density depends upon the description of the collision cross-section. The highly excited atom cross-section and collision linewidth are calculated in the impact approximation, which can be employed in the case when $1.6 \times 10^5\,\mathrm{K}/n^2 T_\mathrm{e} \ll 1$. The collision broadening values ares calculated from equation (3) and listed with the radiation and Doppler widths in table 2.

To find the dimensions of the C II regions, the centimetre radio recombination line intensities are described as functions of the principal quantum number, temperature and amplification factor in equations (5) and (6). The population equations are solved in the analytical diffusion approximation forms represented by equation (5), and the $b_n\beta_n$ factors can be considered versus these numerically calculated values [23, 24]. The centimetre line optical depths were experimentally found in [11, 13] and listed with the temperatures and calculated dimensions for the C II regions in table 3.

Acknowledgements

The author thanks A.A. Konovalenko, L.G. Sodin, V.M. Kontorovich and A.E. Kyrychenko for many useful comments and remarks.

References

[1] W. Li, N.J. Evans, D.T. Jaffe, *et al.*, Astrophys. J. **568** 242 (2002).
[2] A. Natta, C.M. Walmsley and A.G.G.M. Tielens, Astrophys. J. **428** 209 (1994).
[3] M.L. Luhman, S. Satyapal, J. Fischer, *et al.*, Astrophys. J. **594** 758 (2003).
[4] A.G.G.M. Tielens and D. Hollenbach, Astrophys. J. **291** 722 (1985).
[5] A.G.G.M. Tielens and D. Hollenbach, Astrophys. J. **291** 747 (1985).
[6] M.J. Wolfire, A.G.G.M. Tielens and D. Hollenbach, Astrophys. J. **358** 116 (1990).
[7] A.A. Ershov, V.P. Tlyasov, E.E. Leht, G.T. Smirnov and R.L. Sorochenko, Soviet Astron. Lett. **10** 831 (1984).
[8] A.A. Konovalenko, Soviet Astron. Lett. **10** 846 (1984).
[9] A.A. Konovalenko, S.V. Stepkin and D.V. Shalunov, Radiophys. Radioastron. (Ukr.) **6** 21 (2001).
[10] K.R. Anantharamaiah, W.C. Erickson and H.E. Payne, Astrophys. J. **430** 690 (1994).
[11] K.R. Anantharamaiah, N.G. Kantharia and H.E. Payne, Astrophys. J. **506** 758 (1998).
[12] K.R. Anantharamaiah, N.G. Kantharia and W.M. Goss, Astrophys. J. **504** 375 (1998).
[13] N.G. Kantharia and K.R. Anantharamaiah, J. Astrophys. Astron. **22** 51 (2001).
[14] N.I. Rovenskaya, Astrophys. Space Sci. **291** 113 (2004).
[15] M. Brocklehurst and S. Leeman, Astrophys. Lett. **9** 35 (1971).
[16] H.R. Griem, Astrophys. J. **148** 547 (1967).
[17] H.R. Griem, *Spectral Line Broadening by Plasma* (Academic Press, New York, 1974), 491 pp.
[18] P.A. Shaver, Pramana **5** 1 (1975).
[19] L.A. Vainstein, I.I. Sobel'man and E.A. Ukov, *Excitation of Atoms and Spectral Line Broadening* (Nauka, Moscow, 1979), 319 pp.
[20] I.I. Sobel'man, *Introduction to the Atomic Spectrum Theory* (Gosudarstvennoe Izdatel'stvo Fiziko-Matematicheskaya Literatura, Moscow, 1963), 640 pp.
[21] I.L. Beigman, Trud. Fiz. Inst. Akad. Nauk USSR **179** 160 (1987).
[22] I.L. Beigman, *Analytical Methods for Highly Excited Level Populations in Hot Plasma*, edited by R.A. Sunyev (Space Research Institute, Moscow, 2001), 102 pp.
[23] M. Brocklehurst and M. Salem, Astrophys. J., Suppl. Ser. **39** 633 (1979).
[24] N.I. Rovenskaya, Astrophys. Space Sci. **293** 355 (2004).
[25] E.M. Lifshits and L.P. Pitaevskiy, *Physical Kinetics* (Nauka, Moscow, 1979), 527 pp.
[26] S.A. Kaplan and S.B. Pikel'ner, *The Interstellar Medium Physics* (Nauka, Moscow, 1979), 591 pp.
[27] V.O. Ponomarev and R.L. Sorochenko, Sov. Astron. Lett. **18** 541 (1992).
[28] C.M. Walmsley and W.D. Watson, Astrophys. J. **260** 317 (1982).
[29] R.J. Allen, H.I. Heaton and M.J. Kaufman, Astrophys. J. **608** 314 (2004).